X CONGRESSO NACIONAL DE ENGENHARIA MECÂNICA 2018
ABCM
20 A 24 DE MAIO DE 2018 SALVADOR – BA – BRASIL

Uncertainty quantification in the comparison of structural criterions of failure

Yaşar Yanık, ysryanik@gmail.com[1]
Samuel da Silva, samuel@dem.feis.unesp.com[1]
Americo Cunha Jr, americo@ime.uerj.br[2]

[1]Universidade Estadual Paulista - UNESP, Faculdade de Engenharia, Departamento de Engenharia Mecânica, Ilha Solteira, SP, Brasil
[2]Universidade do Estado do Rio de Janeiro - UERJ, Nucleus of Modeling and Experimentation with Computers – NUMERICO, Rio de Janeiro, Brasil

Abstract: *Uncertainty Quantification is a discipline which deals with the quantitative description and reduction of uncertainties in real world applications. It tries to find out how likely certain results are in a few parts of the system are not precisely known. Furthermore, failure theory is the investigation of predicting the circumstances under which solid materials under the processing of external loads. The Failure Theory is known as different failure criteria such as Von Mises and Tresca which are the most famous of these for certain materials. In this context, this paper is going to show a comparison between Tresca and Von Mises failure criterions, taking into account the underlying uncertainties in the constitutive equations and stress analysis.*
Keywords: *failure criterions , stress analysis, uncertainty quantification, parametric probabilistivc approach, Monte Carlo method.*

1. INTRODUCTION

The aim behind the failure criteria is to predict or estimate the yield and failure of machine parts and basic individuals. For the most part the Von Mises and Tresca criteria are demonstrated together with little proposal or discrimination between them in all mechanics of materials books. Furthermore, the primary explanation of the Mises criterion is that it shows a critical value of the distortional energy keeped in the isotropic material while the Tresca criterion is that of a crucial value of the maximum shear stress in the isotropic material (Burns, 2015). Additionally, most of the predictions that are essential for decision making in engineering, financial aspects, actuarial sciences are made in view of computer models. These models depend on presumptions that could be not in accordance with reality. Therefore, a model can have uncertainties on its forecasts, because of conceivable wrong presumptions made during its originations (Cunha Jr, 2015, 2017). Additional varieties may rise from an diversity of sources including the geometry of the issue, material characteristics, limit conditions, starting conditions, or excitations forced on the framework (Wojtkiewicz *et al.*, 2001). The parametric probabilistic approach (Soize, 2012) comprises in modeling the uncertain parameters of the computational model by random variables, in order to construt a stochastic model to deal with the underlying variabilities. This kind of approach is highly fited and and extremely effective to consider the uncertainties on the computational model parameters. Many studies have been published in this area, see Soize (2013) for details.

Once a computational model is contructed, it is necessary investigate how the uncertainties propagate from model parameters to the response. This can be done via Monte Carlo (MC) method, that is the most widely recognized technique for stochastic calculation, because of its simpleness and great factual outcomes. Nevertheless, its computational expense is to a exceedingly, and, as a rule , inhibitive. Luckily the Monte Carlo calculation is effectively parallelizable, which permits its utilization in simulations where the calculation of an individual realization expensive (Cunha *et al.*, 2014). This technique generates several realizations (samples) of the random parameters according to their distributions (stochastic model). Each of these realizations defines a deterministic problem, which is solved (processing) using a deterministic technique, generating an amount of data. Then, all of these data are combined through statistics to access the response of the random system under analysis (Cunha *et al.*, 2014).

In this paper, the quantitication of security factor uncertainties is addressed through a parametric probabilistic approach, using MC as stochastic solver. The goal is to is to verify the effect of the parametric uncertainties in the safety factor obtained with basis on the failure criteria of Mises and Tresca.

2. DETERMINISTIC FAILURE CRITERIONS

At this section, it is shown that the state of plane tension of the mechanical system of interest is defined by the stress tensor

$$\sigma = \begin{bmatrix} \sigma_x & \tau_{xy} \\ \tau_{xy} & \sigma_y \end{bmatrix}, \tag{1}$$

where the parameters σ_x and σ_y are the normal stresses and τ_{xy} is shear stress respectively, being obtained trhough the solution of the eigenvalue problem

$$|[\sigma] - \lambda I|\upsilon = 0, \tag{2}$$

where (λ, υ) is an eigenpair for $[\sigma]$. The obtained eigenvalues are equal to the principal stress values σ_1 and σ_2 used in Von Mises failure criterion,

$$\sigma_{vm} = \sqrt{(\sigma_2 - \sigma_1)^2 + \sigma_1^2 + \sigma_2^2}, \tag{3}$$

and Tresca failure criterion

$$\tau_{tresca} = \sigma_1 - \sigma_2. \tag{4}$$

Thus, the safety factor for Von Mises failure criterion is defined as

$$F_{s(VonMises)} = \frac{\sigma_e}{\sigma_{vm}}, \tag{5}$$

while the safety factor for Tresca failure criterion is given by

$$F_{s(Tresca)} = \frac{\sigma_e}{\sigma_2 - \sigma_1}, \tag{6}$$

where σ_e is the yield stress of the material.

3. SOTOCHASTIC FAILURE CRITERIONS

In this paper, stochastic version of stress matrix is proposed to identify the comparison of structural criterions of failure. The model parameters subjected to uncertainties are described as random variables. Therefore, the system response also becomes a random variable. Therefore, it is shown that the state of plane tension of the mechanical system of interest is defined by stochastic version of the stress tensor

$$\mathfrak{o} = \begin{bmatrix} \mathfrak{o}_x & \mathfrak{t}_{xy} \\ \mathfrak{t}_{xy} & \sigma_y \end{bmatrix} \tag{7}$$

In this part of section, the value of σ_y is given as 2 MPa in the Eq.(8). After giving this value, random values are used by applying uncertainty quantification method considering τ_{xy} and σ_x. Afterward, these values were examined in the non-standard experimental distribution graph considering Maximum Entropy Principle (Kesavan and Kapur, 1989) and the σ values were obtained. Furthermore, stochastic version of the eigenvalue equation is described as shown below

$$|[\mathfrak{o}] - \mathbb{\lambda} I|\upsilon = 0. \tag{8}$$

In addition, while obtaining unknown parameters in these equations, 1024 samples, obtained via Monte Carlo method, are shown on the plot. According to Figs.3, convergence plot of Tresca failure criterion begins to converge after 200 number of samples. At a value of 1024 number of samples, the graph is approximately stable. Moreover, stochastic version of the equation of safety factor for Tresca failure criterion is determined as shown below

$$\mathbb{F}_{s(Tresca)} = \frac{\sigma_e}{\mathfrak{o}_2 - \mathfrak{o}_1}. \tag{9}$$

Stochastic version of stress value for Von Mises will be obtained as shown below

$$\mathfrak{o}_{vm} = \sqrt{(\mathfrak{o}_2 - \mathfrak{o}_1)^2 + \mathfrak{o}_1^2 + \mathfrak{o}_2^2}. \tag{10}$$

After obtaining stochastic version of stress value for Von Mises σ_{vm}, stochastic version of safety factor for Von Mises failure criterion is determined as shown below

$$\mathbb{F}_{s(VonMises)} = \frac{\sigma_e}{\mathfrak{o}_{vm}}. \tag{11}$$

3.1 Maximum Entropy Principle and Convergence Criteria

According to Maximum Entropy Principle, the stochastic equivalent of the approximation shown in Eqs.(12), (13) and (14) are written

$$\int_{-\infty}^{+\infty} p_x(x)dx - 1 = 0, \tag{12}$$

$$\int_{-\infty}^{+\infty} xp_x(x)dx - \mu = 0, \tag{13}$$

$$\int_{-\infty}^{+\infty} x^2p_x(x)dx - \mu^2 - \sigma^2 = 0, \tag{14}$$

where $p_x(x)$ is probability density function of the random parameter. When these three equations, (12), (13) and (14) are solving, it is also assumed that support, μ (mean) and σ (variance) of the random variables are known.

$$p_x(x) = e^{-\lambda_0}e^{-\lambda_1 x - \lambda_2 x^2} \tag{15}$$

where λ_0, λ_1 and λ_2 are the solution the Eqs.(12), (13) and (14). Considering Eqs.(12), (13) and (14), the values of $\sigma_x^{(max)}$ and $\tau_{xy}^{(max)}$, $\sigma_x^{(min)}$ and $\tau_{xy}^{(min)}$ are given as 280 kPa and 120 kPa separetely for solving these equations in stochastic way for σ_x and τ_{xy} random variables. Also, μ (mean) and σ (variance) values of the σ_x and τ_{xy} are given as 200 kPa and 280 kPa respectively for solving these equations. After giving these values, the variables λ_0, λ_1 and λ_2 were obtained. These variables λ_0, λ_1 and λ_2 equal to -75.162, -0.71425 and 0.00178564 respectively for solving these non-linear equations.

Furthermore, the mean-square convergence analysis (Cataldo *et al.*, 2009) with respect to independent realizations $F_{s(Tresca)}$ (θ_1),..., $F_{s(Tresca)}$ (θ_n) of the random variable $F_{s(Tresca)}$ is carried out studying the function $n \longmapsto Conv(n)$ defined by

$$Conv(n) = \frac{1}{n}\sum_{j=1}^{n} F_{s(Tresca)}(\theta_j)^2 \tag{16}$$

Also, non-standard experimental distribution graphs are described for solving the stress tensor considering σ_x normal stress and τ_{xy} shear stress shown in Figure 1.

Figura 1: The comparison between generated and theoretical non-standard distrubution

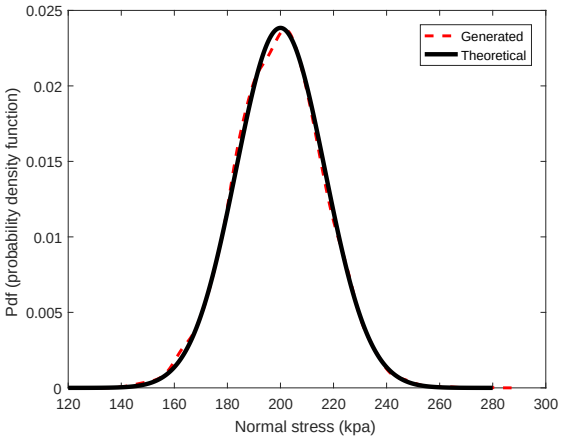

Source: Source made by the author

4. RESULTS AND DISCURSSION

According to the probability density function graph Figs. 3, the F_s values were obtained in the Von Mises and Tresca equations, and Von Mises and Tresca failure criterion methods were compared. Furthermore, after obtaining the probability density function graph Figs. 3, a convergence graphic Figs. 2 between Von Mises and Tresca was acquired too. Also, in the range of 2.75 F_s (Safety Factor), the plots of probability density function for failure criterions intersect in each other according to the probability density function graph Figs. 3

Figura 2: Convergence of the Tresca failure criterion

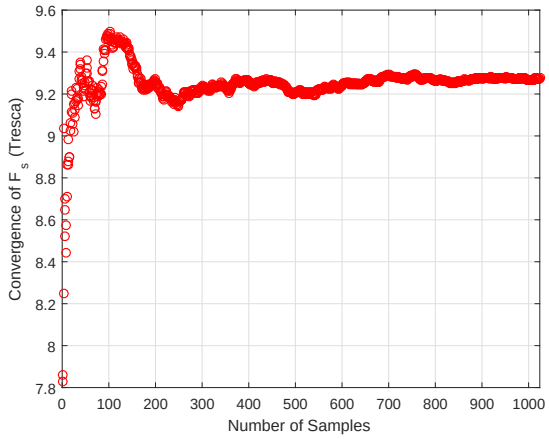

Source: Source made by the author.

The probability density function that was obtained according to the Von Mises and Tresca criterion using Eq.(6), is interpreted, the blue and pink colors describe Tresca failure criterion and Von Mises failure criterion, respectively. According to Figs. 3, in the range of 2.0-3.5 F_s (Safety Factor), the areas where Von Mises and Tresca failure criterion have a common value range.

Figura 3: Probablility Density function and Histogram for Von Mises and Tresca

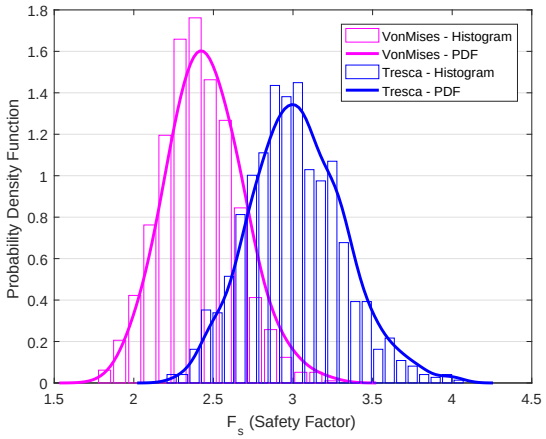

Source: Source made by the author.

In addition, the closest match between Von Mises and Tresca failure criterion is in the range of 2.7 F_s (Safety Factor). Also, there is no common intersection area between Von Mises and Tresca failure criterion in the range of 1.5-2.0 F_s (Safety Factor) and 3.5-4.3 F_s (Safety Factor), respectively. It is seen that Von Mises and Tresca failure criterion are not different from each other according to Figs. 3

4.1 Results and Discussion Considering Two Uncertainties

In this part of the section, the random parameters τ_{xy} and σ_x are independent in each other. According to the probability density function graph Figs. 4, the F_s values were obtained in the Von Mises and Tresca equations, and Von Mises and Tresca failure criterion methods were compared. Furthermore, after obtaining the probability density function graph Figs. 4, a convergence graphic Figs. 5 between Von Mises and Tresca was acquired too. Also, in the range of 2.65 F_s (Safety Factor), the plots of probability density function for failure criterions intersect in each other according to the probability density function graph Figs. 4.

Figura 4: Probability Density Function and Histogram for Von Mises and Tresca considering two uncertainties

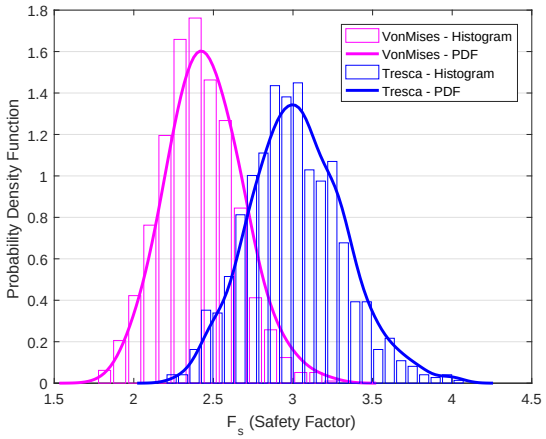

Source: Source made by the author.

According to convergence graph Figs. 5, 250000 number of samples are expressed by using Maximum Entropy Principle and shown on the plot. Convergence plot of Tresca failure criterion begins to converge after 10000 number of samples. At a value of 250000 number of samples, the graph is approximately stable.

Figura 5: Convergence of the Tresca failure criterion considering two uncertainties

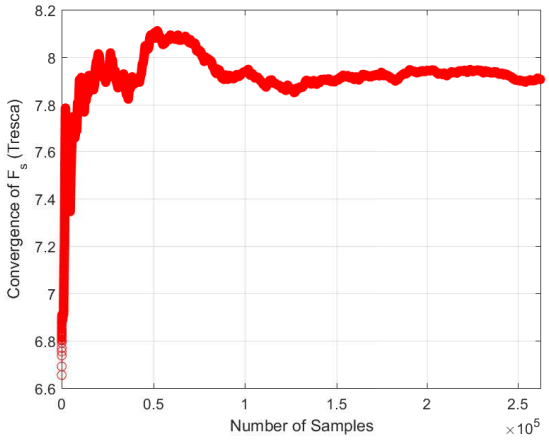

Source: Source made by the author.

The convergence plot that was obtained according to Tresca criterion using Eq.(5), is to be interpreted. In the range of 0-10000 number of samples, Tresca failure criterion is irregularly distant from each other according to Figs. 5. Furthermore, in the range of 10000-250000 number of samples, convergence values between Tresca failure criterion was found to approach each other

4.2 The Simple Deflection Problem Considering Uncertainty Quantification

The cantilever beam AB is uniform cross section and carries a load F at it is free and end at the point of A. The equation of the elastic curve and the deflection and slope at A were determined as shown below (Beléndez *et al.*, 2002).

$$\frac{d^2v}{dx^2} = \frac{M(x)}{EI} \tag{17}$$

Using the free-body diagram of the portion AB of the beam according to Figs. 6, if the equation is determined as shown below

$$M(x) = F\,(L - x) \tag{18}$$

if the equation integrate Eq.(18) considering variable x, the equation will be obtained as shown below

$$EI\frac{dv}{dx} = FLx - \frac{1}{2}Fx^2 + C_1 \tag{19}$$

We now observe that at the fixed end B we have v(0) = 0 and θ = dv/dx = 0. Substituting these values into Eq.(19) and solving for C_1, then C_1 is determined as shown below

$$C_1 = 0 \tag{20}$$

Figura 6: Deflection Beam

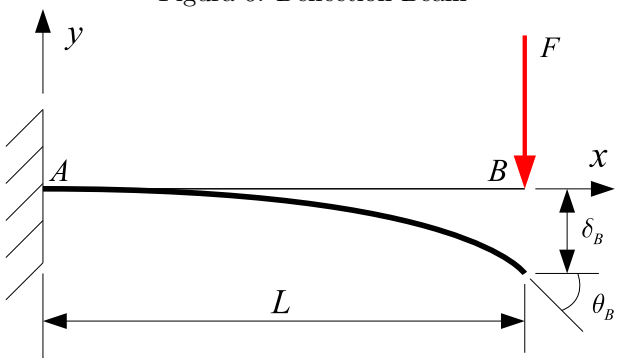

Integrating both members of Eq.(19), then the equation is determined as shown below

$$EIv = \frac{1}{2}FLx^2 - \frac{1}{6}Fx^3 + C_2 \tag{21}$$

But, at B we have x = L , y = 0. Substituting into Eq.(21), then the equation is determined as shown below

$$\frac{1}{2}FLx^2 - \frac{1}{6}Fx^3 + C_2 = 0 \tag{22}$$

$$C_2 = 0 \tag{23}$$

Carrying the value of C_2 back into Eq.(21), then the equation of the deflection function is determined as shown below

$$v(x) = \frac{1}{EI}\left(\frac{1}{2}FLx^2 - \frac{1}{6}Fx^3\right) \tag{24}$$

The boundary conditions are that the displacement and slope are both zero at clamped and from which the two constant of integration can be obtained. Then, the slope function will be maximum at x = L, the equation of the slope function is determined as shown below

$$\frac{dv}{dx} = \frac{1}{EI}\left(FLx - \frac{1}{2}Fx^2\right) \tag{25}$$

$$\frac{dv}{dx} = \frac{1}{EI}\left(\frac{1}{2}FL^2\right) \tag{26}$$

Afterward, the Hooke-Lamé's Law in Cartesian Coordinates were examined and the σ_x values were obtained. In this part of the work, the Hooke-Lamé's Law in Cartesian Coordinates were examined in a deterministic way considering ε_x displacement and other variables were eliminated. After that, the eliminated equation of Hooke-Lamé's Law in Cartesian Coordinates is determined as shown in Eq.(28)

$$\begin{bmatrix} \sigma_x \\ \sigma_y \\ \sigma_z \\ \tau_{xy} \\ \tau_{xz} \\ \tau_{zy} \end{bmatrix} = \begin{bmatrix} \lambda+2G & \lambda & \lambda & 0 & 0 & 0 \\ \lambda & \lambda+2G & \lambda & 0 & 0 & 0 \\ \lambda & \lambda & \lambda+2G & 0 & 0 & 0 \\ 0 & 0 & 0 & G & 0 & 0 \\ 0 & 0 & 0 & 0 & G & 0 \\ 0 & 0 & 0 & 0 & 0 & G \end{bmatrix} \begin{bmatrix} \varepsilon_x \\ \varepsilon_y \\ \varepsilon_z \\ \gamma_{xy} \\ \gamma_{xz} \\ \gamma_{zy} \end{bmatrix} \tag{27}$$

$$\begin{bmatrix} \sigma_x \end{bmatrix} = \begin{bmatrix} \lambda+2G \end{bmatrix} \begin{bmatrix} \varepsilon_x \end{bmatrix} \tag{28}$$

The slope function at x = L will be equal to displacement ε_x.

$$\frac{dv}{dx} = \varepsilon_x = \frac{1}{EI}\left(\frac{1}{2}FL^2\right) \tag{29}$$

In the Hooke-Lamé's Law in Cartesian Coordinates, shear (G) and lambda (λ) modulus were determined (Landau and Lifshitz, 1970) as shown in Eqs.(30) and (31) for explain to σ_x normal stress

$$\lambda = \frac{\nu E}{(1+\nu)(1-2\nu)} \tag{30}$$

$$G = \frac{E}{2(1+\nu)} \tag{31}$$

Also, moment of inertia of cantilever beam is determined as shown in Eq.(32) below (Landau and Lifshitz, 1970; Timoshenko, 1983; Beléndez *et al.*, 2001).

$$I = \int y^2 dA = \int_{-h/2}^{+h/2} y^2 dy = \frac{bh^3}{12} \tag{32}$$

Tabela 1: Parameters used in Hooke-Lamé's equation in a deterministic way

$E[Pa]$	ν	$h[m]$	$b[m]$	$L[m]$	$\sigma_e[Pa]$
$210 * 10^9$	0.3	0.025	0.05	1	$5 * 10^9$

In this part of the section, where the parameters of stress matrix are E (elastic module) , I (moment of inertia), F (force) and L (length of beam) respectively according to Eq.(26) slope function, the value of E and L are given as $210 * 10^9 Pa$ and $1m$ for solving the equation in a deterministic way

4.3 Stochastic Explanation for the Simple Deflection Problem

In this part of the section, non-standard experimental distribution graph is used for solving the stress tensor and the simple deflection problem instead of γ distribution graph. Because, when the negative values are used for normal stress σ_x and Force F. Non-standard experimental distribution graph should be used considering Maximum Entropy Principle. After that, random variables τ_{xy} and σ_x are considered for stress matrix. The process is repeated until the convergence is achieved.
Furthermore, the parameters F for the equation of the slope function are considered as random variables according to simple beam deflection problem. Afterward, these parameters were examined in the non-standard experimental distribution graph considering Maximum Entropy Principle (Pavon and Ferrante, 2013).

Using the free-body diagram of the portion AB of the beam according to Figs. 6, if the stochastic version of equation is determined as shown below

$$\mathbb{M}(x) = \mathbb{F}\,(L - x) \tag{33}$$

if the equation integrate Eq.(33) considering variable x, the equation will be obtained as shown below

$$EI\frac{d\mathbb{v}}{dx} = \mathbb{F}Lx - \frac{1}{2}\mathbb{F}x^2 + C_1 \tag{34}$$

Integrating both members of Eq.(32), then the stochastic version of equation is determined as shown below

$$EI\mathbb{v} = \frac{1}{2}\mathbb{F}Lx^2 - \frac{1}{6}\mathbb{F}x^3 + C_2 \tag{35}$$

Carrying the value of C_2 back into Eq.(35), then the stochastic version of the deflection function is determined as shown below

$$\mathbb{v}(x) = \frac{1}{EI}\left(\frac{1}{2}\mathbb{F}Lx^2 - \frac{1}{6}\mathbb{F}x^3\right) \tag{36}$$

The slope function will be maximum at x = L, the equation of the stochastic version of slope function is determined as shown below

$$\frac{d\mathbb{v}}{dx} = \frac{1}{EI}\left(\mathbb{F}Lx - \frac{1}{2}\mathbb{F}x^2\right) \tag{37}$$

$$\frac{d\mathbb{v}}{dx} = \frac{1}{EI}\left(\frac{1}{2}\mathbb{F}L^2\right) \tag{38}$$

After that, the eliminated the stochastic version of Hooke-Lamé's equation is determined as shown in Eq.(39)

$$\left[\ \mathbb{\sigma}_x\ \right] = \left[\ \lambda + 2G\ \right]\left[\ \mathbb{\xi}_{x_x}\ \right] \tag{39}$$

The stochastic version of slope function at x = L will be equal to displacement ε_x.

$$\frac{d\mathbb{v}}{dx} = \mathbb{\xi}_x = \frac{1}{EI}\left(\frac{1}{2}\mathbb{F}L^2\right) \tag{40}$$

Considering Eqs.(12), (13) and (14), the values of F_{max} and F_{min} are given as 350N and 150N separetely for solving these equations in stochastic way. Also, μ (mean) and σ (variance) values of the force are given as 250N and 350 N respectively for solving these equations. After giving these values, the variables λ_0, λ_1 and λ_2 were obtained in Matlab. These variables λ_0, λ_1 and λ_2 equal to -93.1334, -0.71428 and 0.0014286 respectively for solving these non-linear equations.

Also, non-standard experimental distribution graphs are described for solving the simple deflection problem shown below

Figura 7: The comparison between generated and theoretical non-standard distrubution

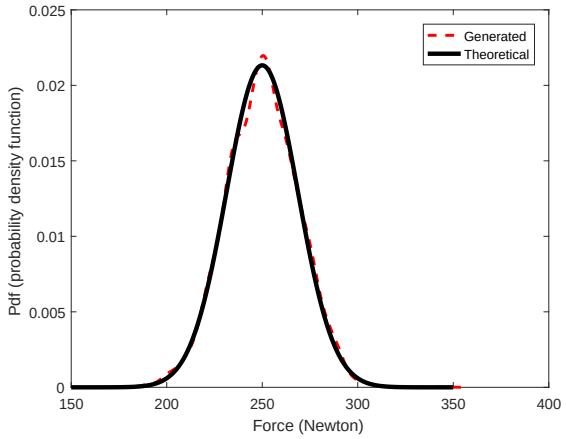

Source: Source made by the author

4.4 Results and Discussion for Simple Deflection Problem

While obtaining unknown parameters in these equations, 8192 number of samples are described by using generalized maximum entropy principle and shown on the plot. According to Figs. 8, convergence plot of Tresca failure criterion begins to converge after 1000 number of samples. At a value of 8192 number of samples, the graph is approximately stable

Figura 8: Convergence of the Tresca failure criterion considering two uncertainties

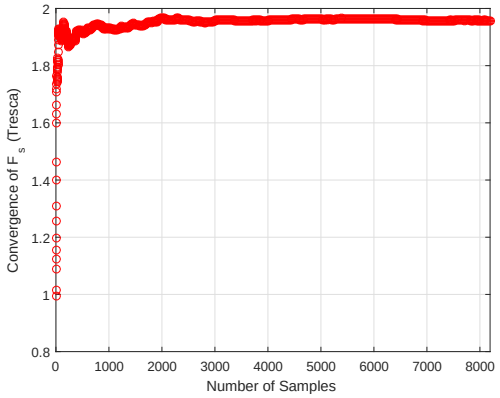

In addition, according to Figs. 9, these graph shows that comparison between Von Mises and Tresca failure criterion of probability density functions. In addition, the closest match between Von Mises and Tresca failure criterion is in the range of 1.18 F_s (Safety Factor). Also, there is no common intersection area between Von Mises and Tresca failure criterion in the range of 0.8-0.96 F_s (Safety Factor) and 1.36-1.93 F_s (Safety Factor). As a result, Von Mises and Tresca failure criterion has many common intersection areas in the range of 1.1-1.36 F_s (Safety Factor) and it is seen that Von Mises and Tresca failure criterion are not different from each other according to Figs. 9 considering uncertainty quantification method for F

5. FINAL REMARKS

The using of Von Mises and Tresca failure criterions can help the investigation of predicting the circumstances under which solid materials under the processing of external loads. The results obtained in the present paper have shown the comparison between Von Mises and Tresca failure criterions by taking into the consideration with Monte Carlo Simulations and Maximum Entropy Principle. Based on the results shown, the failure criterions investigated here can be useful in applications for the identification and analysis of stress analysis. Future steps

Figura 9: Probability Density Function and Histogram for Von Mises and Tresca considering two uncertainties

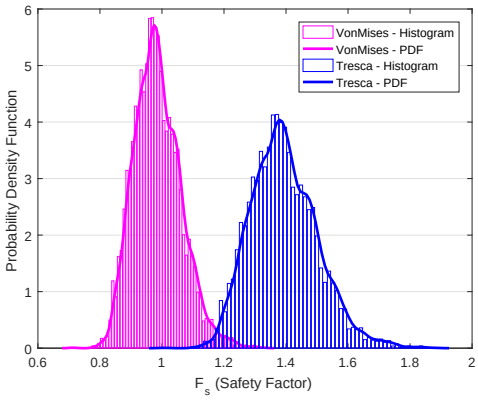

of this research are concerned with applications involving comparison between failure criterions by taking into uncertainty quantifications

6. ACKNOWLEDGMENTS

The authors would like to thank the financial support provided by CAPES, CNPq, FAPESP, FAPERJ.

7. REFERENCES

Beléndez, A., Neipp, C. and Beléndez, T., 2001. "Experimental study of the bending of a cantilever beam". *Rev. Esp. Fis*, Vol. 15, No. 3, pp. 42–5.

Beléndez, T., Neipp, C. and Beléndez, A., 2002. "Large and small deflections of a cantilever beam". *European Journal of Physics*, Vol. 23, No. 3, p. 371. URL `http://stacks.iop.org/0143-0807/23/i=3/a=317`.

Burns, S.J., 2015. "The theory of materials failure, by richard m. christensen: Scope: monograph. level: postgraduate, advanced undergraduates".

Cataldo, E., Soize, C., Sampaio, R. and Desceliers, C., 2009. "Probabilistic modeling of a nonlinear dynamical system used for producing voice". *Computational Mechanics*, Vol. 43, No. 2, pp. 265–275.

Cunha, A., Nasser, R., Sampaio, R., Lopes, H. and Breitman, K., 2014. "Uncertainty quantification through the monte carlo method in a cloud computing setting". Vol. 185, pp. 1355–1363. doi: http://dx.doi.org/10.1016/j.cpc.2014.01.006.

Cunha Jr, A., 2017. "Modeling and Quantification of Physical Systems Uncertainties in a Probabilistic Framework". In S. Ekwaro-Osire, A.C. Goncalves and F.M. Alemayehu, eds., *Probabilistic Prognostics and Health Management of Energy Systems*, Springer International Publishing, pp. 127–156. doi: http://dx.doi.org/10.1007/978-3-319-55852-3_8.

Cunha Jr, A., 2015. *Modeling and Uncertainty Quantification in the Nonlinear Stochastic Dynamics of Horizontal Drillstrings*. Theses, Université Paris-Est (UPE), Pontifícia Universidade Católica do Rio de Janeiro (PUC-Rio). URL `https://hal-upec-upem.archives-ouvertes.fr/tel-01134041`.

Kesavan, H.K. and Kapur, J.N., 1989. "The generalized maximum entropy principle". *IEEE Transactions on systems, Man, and Cybernetics*, Vol. 19, No. 5, pp. 1042–1052.

Landau, L. and Lifshitz, E., 1970. "Theory of elasticity, vol. 7 of course of theoretical physics, 2nd english ed".

Pavon, M. and Ferrante, A., 2013. "On the geometry of maximum entropy problems". *SIAM review*, Vol. 55, No. 3, pp. 415–439.

Soize, C., 2013. "Stochastic modeling of uncertainties in computational structural dynamics - recent theoretical advances". *Journal of Sound and Vibration*, Vol. 332, No. 10, pp. 2379 – 2395. doi: http://dx.doi.org/10.1016/j.jsv.2011.10.010.

Soize, C., 2012. *Stochastic models of uncertainties in computational mechanics*. American Society of Civil Engineers Reston.

Timoshenko, S.P., 1983. *History of strenght of materials: with a brief account of the history of theory of elasticity and theory of structures*.

Wojtkiewicz, S., Eldred, M., Field, Jr, R., Urbina, A. and Red-Horse, J., 2001. "Uncertainty quantification in large computational engineering models". In *19th AIAA Applied Aerodynamics Conference*. p. 1455.

8. AUTHORS RESPONSIBILITY

The authors are the only one responsible for the content of this work.